Catena 149 (2017) 221–231

Contents lists available at ScienceDirect

Catena

journal homepage: www.elsevier.com/locate/catena

Potential CO_2 emissions from defrosting permafrost soils of the Qinghai-Tibet Plateau under different scenarios of climate change in 2050 and 2070

Anna Bosch [a,*], Karsten Schmidt [a], Jin-Sheng He [b,c], Corina Doerfer [a], Thomas Scholten [a]

[a] University of Tuebingen, Department of Geosciences, Chair of Soil Science and Geomorphology, Tübingen, Germany
[b] Key Laboratory of Adaptation and Evolution of Plateau Biota, Northwest Institute of Plateau Biology, Chinese Academy of Sciences, Xining 810008, China
[c] Department of Ecology, College of Urban and Environmental Sciences, Key Laboratory for Earth Surface Processes of the Ministry of Education, Peking University, Beijing 100871, China

ARTICLE INFO

Article history:
Received 3 February 2016
Received in revised form 22 July 2016
Accepted 29 August 2016
Available online xxxx

Keywords:
Permafrost soil
Carbon
Carbon dioxide
Soil respiration
Qinghai-Tibet Plateau
Climate change scenarios

ABSTRACT

Permafrost soils store enormous quantities of organic carbon. Especially on the alpine Qinghai-Tibet Plateau, global warming induces strong permafrost thawing, which strengthens the microbial decomposition of organic carbon and the emission of the greenhouse gas carbon dioxide (CO_2). Enhanced respiration rates may intensify climate warming in turn, but the magnitude of future CO_2 emissions from this data-scarce region in a changing climate remains highly uncertain. Here, we aim at an area-wide estimation of future potential CO_2 emissions for the permafrost region on the Qinghai-Tibet Plateau as key region for climate change studies due to its size and sensitiveness. We calculated four potential soil respiration scenarios for 2050 and 2070 each. Using a regression model, results from laboratory experiments and C stock estimations from other studies, we provide an approximation of total potential soil CO_2 emissions on a regional scale ranging from 737.90 g CO_2 m^{-2} y^{-1}–4224.77 g CO_2 m^{-2} y^{-1}. Our calculations as first estimate of thawing-induced CO_2 emissions (51.23 g CO_2 m^{-2} y^{-1}–3002.82 g CO_2 m^{-2} y^{-1}) from permafrost soils of the Qinghai-Tibet Plateau under global warming appear to be consistent to measurements of C loss from thawing permafrost soils measured within other studies. Thawing-induced soil CO_2 emissions from permafrost soils with a organic C content ranging from 2.42 g C kg^{-1} to 425.23 g C kg^{-1} increase general soil respiration by at least about one third on average at a temperature of 5 °C. Differences between scenarios remain <1% and thawing-induced CO_2 emissions generally decrease over time comparing 2015, 2050 and 2070. With this spatial approximation at a regional scale, a first area-wide estimate of potential CO_2 emissions for 2050 and 2070 from permafrost soils of the Qinghai-Tibet Plateau is provided. This offers support of assessing potential area-specific greenhouse gas emissions and more differentiated climate change models.

1. Introduction[1]

Carbon dioxide (CO_2) emissions from soils to the atmosphere substantially affect the global carbon (C) cycle (Chen et al., 2010). For the global carbon budget, this soil efflux represents the main source of C, second to oceans´ releases, by approximated 98 ± 12 Pg C per year (Bond-Lamberty and Thomson, 2010a; Schlesinger and Andrews, 2000; Valentini et al., 2000). Further, soils store most carbon in terrestrial ecosystems (Amundson, 2001) and their respiration amounts to ~10% of the atmospheric CO_2 cycle budget (Bond-Lamberty and Thomson, 2010b). Hence, slight increases in soil CO_2 emissions can seriously impact atmospheric CO_2 concentrations, possibly amplifying global warming (Rodeghiero and Cescatti, 2005; Rodeghiero et al., 2013; Davidson and Janssens, 2006; Schlesinger and Andrews, 2000). However, climate warming itself presumably accounts for the rising global loss of soil carbon to the atmosphere in the main (Jones et al., 2003). It potentially increases belowground biomass (BGB), which in turn increases autotrophic respiration and probably also stimulates microorganisms which accordingly leads to a higher heterotrophic respiration supported by more exudates and C-input of roots (Kirschbaum, 1995; Wang et al., 2014a). However, especially higher C loss through augmented autotrophic respiration as consequence of an elevated rate of photosynthesis is expected to be neutralized by a higher plant uptake of C and its sequestration (Schuur et al., 2015). Higher temperatures, extended growing seasons and a higher concentration of atmospheric CO_2 potentially intensify plant growth (Shaver et al., 2000). Uptaken C can be sequestered in larger above- and belowground biomass (Sistla et al., 2013).

* Corresponding author at: University of Tuebingen, Department of Geosciences, Soil Science and Geomorphology, Ruemelinstraße 19-23, D-72070 Tübingen, Germany.
E-mail address: anna.bosch@geographie.uni-tuebingen.de (A. Bosch).

[1] Abbreviations: soil respiration (SR), carbon (C), carbon dioxide (CO2), mean annual precipitation (MAP), representative concentration pathway (RCP), belowground biomass (BGB).

http://dx.doi.org/10.1016/j.catena.2016.08.035
0341-8162/

Understanding the different responses of autotrophic and heterotrophic respiration to global warming in permafrost soils is particularly important (Hicks Pries et al., 2013). Higher soil CO_2 emissions resulting from thawing permafrost are, if at all, only partly offset by this negative feedback to global warming through enhanced soil respiration (Schuur et al., 2015). Permafrost is commonly defined as ground (soil or rock and included ice or organic material) at or below 0 °C for at least two consecutive years. Temperatures at or below 0 °C in permafrost soils shrink microbial activity and inhibits active microbial decomposition of the soil´s accumulated organic matter (Harden et al., 1992). Consequently, warmer temperatures and concomitant thawing of permafrost resulting from climate change will expose a large amount of soil organic C to microbial breakdown that has been frozen before (Xue et al., 2016; Schuur et al., 2009). As a result, high quantities of C may be released to the atmosphere (Dutta et al., 2006). Lately, permafrost was estimated to contain more than 1600 Pg soil organic C (Schuur et al., 2008), which is twice the atmospheric CO_2-C pool (Jia et al., 2006). Considering the remarkable C stock of permafrost and its wide-spread climate change induced degradation, its soil CO_2 emissions are of global importance in view of the greenhouse gas-driven climate change (Schaefer et al., 2011; Ding et al., 2016). Hence, the quantification of future CO_2 emissions from permafrost soil gains high relevance for more comprehensive scenarios of climate change. This importance further results from the fact that permafrost soils have functioned as C sinks so far (Hicks Pries et al., 2012).

A key region for examining such processes due to its sensitivity and comparably low human impact is seen in the ecologically fragile Qinghai-Tibet Plateau with its extensive and sensitive permafrost area (Fan et al., 2010; Yang et al., 2009; Liu and Chen, 2000). Also because of its important role in the global carbon cycle and remarkable contribution to the global carbon budget, the plateau is generally of high significance for studies on CO_2 emissions (Geng et al., 2012). As highest and spatially most extended plateau on earth, the Qinghai-Tibet Plateau influences both regional and global climates significantly (Zhong et al., 2010; Wang et al., 2006). Also its effects by means of thermal and mechanical forces (Kutzbach et al., 2008; Duan and Wu, 2005; Manabe and Terpstra, 1974) earns him the reputation of being a 'driving force' or an 'amplifier' of global warming (Kang et al., 2010). However, global climate change likewise influences the Qinghai-Tibet Plateau (Zhang et al., 2010). It is a region of high sensitiveness to global warming mainly due to its extreme elevation (Zhong et al., 2010; Zhang et al., 2007; Luo et al., 2002). The plateau´s temperature is expected to increase far above average in the future (Wang et al., 2008; Christensen et al., 2007; Liu and Chen, 2000). The cryosphere, commonly considered as the most sensitive indicator to climate change, undergoes rapid changes on the Qinghai-Tibet Plateau (Kang et al., 2010), where earth´s largest high-altitude and low-latitude permafrost zone, with more than half of its total area influenced by permafrost (Cheng, 2005), shows increasing permafrost degradation (Böhner and Lehmkuhl, 2005; Baumann et al., 2009). This process has been advancing even stronger than in other high-latitude, low-altitude permafrost regions over the last few decades (Yang et al., 2004). As expected, the further degradation of Tibetan permafrost (Böhner and Lehmkuhl, 2005; Wang et al., 2000) will highly influence soils mainly reflected by their changes in temperature and moisture (Doerfer et al., 2013; Zhang et al., 2003). Global warming so impacts permafrost stability and distribution as well as vegetation and soil characteristics that intensively interact with CO_2 emissions through complex processes (Chapin et al., 2005). The thaw of permafrost resulting from global warming will release organic C frozen till then and potentially provide a positive feedback to climate change through higher respiration rates (Koven et al., 2011). This calls attention to the need of a deep understanding of the quantity of potential CO_2 emission rates with future climate change with special regard to the heterotrophic component in thawing permafrost soils on the Qinghai-Tibet Plateau (Geng et al., 2012). This is especially difficult to quantify because of high uncertainties and only few laboratory experiments that have been conducted so far concerning thawing-induced CO_2 emissions from permafrost. Widely varying approximations have not been overcome yet (Lawrence et al., 2015). Empirical regression models for predicting soil respiration on the Qinghai-Tibet Plateau have already been applied effectively (Bosch et al., 2016), with process-based models generally being limited in their applicability to large regions due to more difficulties when parametrizing. This approach has been successful when applied for likewise complex processes such as rainfall erosivity in other regions of China (e.g. Schönbrodt-Stitt et al., 2013). For thawing-induced CO_2 emissions, no formulated regression models exist, why results of laboratory experiments are transferred to the study area in structural analogy to regression models. Further, as to the difficulty of quantifying soil CO_2 emissions on the Qinghai-Tibet Plateau, limitations in data availability is particularly challenging. Despite its unique role in climate change studies due to its ecological sensibility, the inaccessible and complex terrain of the plateau additionally aggravates research activities and causes a general data scarcity due to enormous time and cost efforts required for data collection. Various data sets lack of a fine (about 1 km^2) resolution that captures spatial environmental variability appropriately. Others are not spatially comprehensive, existent, available or highly cost-intensive. On the other hand, several freely available global databases exist for selected environmental variables. They are have often acceptable or useful resolution to reasonably interpret empirical model results (about 1 km^2) and are developed through the harmonization of different data sets with elaborated methods. For area-explicit, efficient calculations for the Qinghai-Tibet Plateau on a regional scale, they are, therefore, advantageous.

Facing these issues, we aim at a first, efficient estimate of potential CO_2 emissions from permafrost soils on the Qinghai-Tibet Plateau in future based on freely accessible data. Against the background of different scenarios of climate change, the potential CO_2 release is approximated with special regard to the higher heterotrophic respiration induced by the increased microbial decomposition of soil organic C resulting from thawing permafrost.

2. Material and methods

2.1. Study area

Our study area, the permafrost soils on the Qinghai-Tibet Plateau, is located in southwestern China. The Qinghai-Tibet Plateau extends from 26°00′12″ N to 39°46′50″ N and from 73°18′52″ E to 104°46′59″ E with a maximum length of approx. 2945 km from east to west and approx. 1532 km from south to north. The altitude of the highest and youngest plateau amounts to 4380 m on average (Baumann et al., 2009; Zhang et al., 2002). On this plateau, earth´s largest high-altitude and low-latitude permafrost zone is located, with more than half of its total area influenced by permafrost (Cheng, 2005). Covering about 1.050×10^6 km^2, the permafrost zone is mainly part of the southwestern and central plateau (Fig. 1). Continuous permafrost mostly occurs in the interior and western Qinghai-Tibet Plateau, extending to the south of the Kunlun Mountains. Boundaries of the permafrost zone in the south are the Tanggula Mountains and the 94° longitude in the east. Discontinuous permafrost can be found in the northern and southern regions on the Qinghai-Tibet Plateau with more pronounced relief characterized by ground that seasonally freezes and shows sporadic permafrost (Cheng and Jin, 2013). Along the Qinghai-Tibet highway, the permafrost zones stretches with a length of 550 km from north to south (Wang et al., 2006). The unique geographical position of the Qinghai-Tibet Plateau prevails an azonal plateau climate (Zhuang et al., 2010; Zhong et al., 2010) with strong solar radiation, low air temperature, large daily temperature variations and low differences between annual mean temperatures (Zhong et al., 2010). Generally, a decrease both in temperature and in precipitation from the south-eastern to the north-western part of the plateau is apparent (Immerzeel et al., 2005). For the plateau, the mean temperature of July, as warmest month, varies from 7 °C to

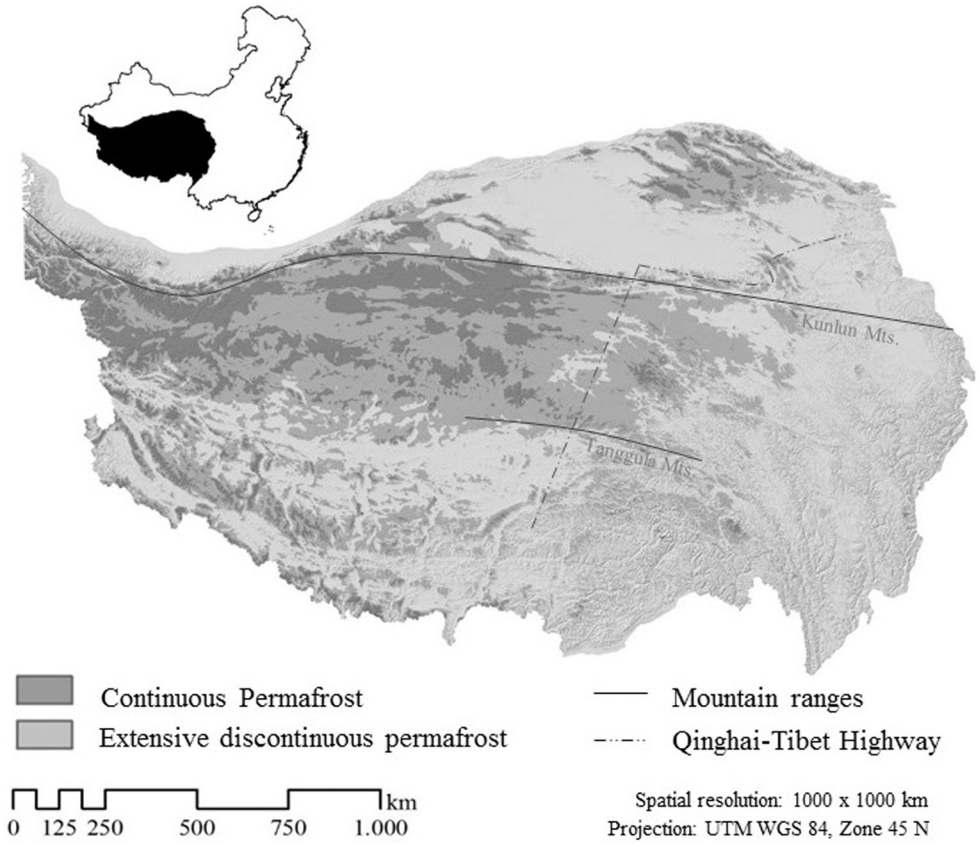

Fig. 1. Spatial extension of continuous and extensive discontinuous permafrost on the Qinghai-Tibet Plateau. The spatial resolution of the grids is 1000 × 1000 m.

15 °C and from −1 °C to −7 °C in January, as coldest month. Average annual temperature is 1.6 °C (Yang et al., 2009). Precipitation amounts to about 413.6 mm a year (Yang et al., 2009), with more than 60–90% falling in the wet and humid summers (June–September) and 10% at maximum in the cool, arid winters (November–February) (Xu et al., 2008). The topographic setting as well as atmospheric conditions determine the sequence of alpine meadows, steppes and deserts from southeast to northwest (Pei et al., 2009; Zheng, 1996). Alpine steppes and meadows dominate the undisturbed vegetation, with *Stipa* species respectively *Kobresia* meadows as major vegetation types. According to the long freezing periods, relatively short growing seasons characterize the plateau`s climate (Yu et al., 2010). Its vegetation is regarded as comparatively natural (Schroeder and Winjum, 1995). Continuous, complex pedogenetic processes on the Qinghai-Tibet Plateau typically result in young and highly diverse soils with distinct degradation characteristics, exhibiting a strong influence by permafrost regimes (Baumann et al., 2014).

2.2. Geodatabase and processing

For the estimation of potential CO_2 emissions, different data sets were used in this case study. All data sets were projected into the Universal Transverse Mercator coordinate system WGS 1984, Zone 45 N. The data set for current MAP was obtained from the WorldClim data set available at http://worldclim.com (for basic statistics on current MAP see Table 1). This was compiled from a considerable number of various sources, such as the Global Historical Climate Network, World Meteorological Organization and the Food and Agricultural Organization, with a resolution of 1 × 1 km and representing the current climate conditions from circa 1950 to 2000. Data from more than 71,000 climate stations worldwide recording for precipitation, and more than 45,000 climate stations recording for temperature are integrated, with the Qinghai-Tibet Plateau as area with less densely distributed measurement points. These were, however, interpolated using a thin-plate smoothing spline algorithm. Latitude, longitude and altitude served as independent variables. Elevation data were used from the Shuttle Radar Topography Mission with a spatial resolution of 1 × 1 km (for more detailed information see Hijmans et al., 2005).

The data sets for MAP in 2050 and 2070 under different scenarios of climate change originate from the WorldClim data sets as well (for basic statistics on MAP in 2050 and 2070 under different scenarios see Table 1). For 2050 and 2070, representing the average of modeled climate conditions from 2041 to 2060 and 2061–2080, respectively, there are four climate scenarios. We used the projections of the global climate model 'Community Climate System Model Version 4' as one of the

Table 1
Statistics on input data sets on MAP [mm] based on WorldClim data sets (Hijmans et al., 2005).

Year scenario	2015	2050 RCP2.6	2050 RCP4.5	2050 RCP6.0	2050 RCP8.5	2070 RCP2.6	2070 RCP4.5	2070 RCP6.0	2070 RCP8.5
					[mm]				
Mean	222.05	232.49	235.13	233.69	241.79	231.78	234.98	235.36	243.44
Min	32.36	35.36	34.58	35.08	35.44	34.40	33.36	35.40	36.40
Max	1237.18	1291.94	1287.11	1261.01	1243.34	1295.14	1338.14	1247.18	1303.71
Range	1204.82	1256.58	1252.53	1225.93	1207.9	1260.74	234.98	1211.78	1267.31
SD	137.67	143.70	145.73	144.207	148.66	143.81	147.32	145.33	151.12

most common and current one that is employed in the Fifth Assessment IPCC report as well and has been developed in international collaboration (Gent et al., 2011). The model is a coupled model combining four separate models that simulate the sea-ice, the atmosphere, oceans and land surface of the earth, and a fifth component that allows for an exchange of fluxes between these models. It is regarded to provide realistic simulations of the earth´s climate system at a resolution of 1 × 1 km with reasonable fidelity. WorldClim 1.4 served as reference for the downscaling and calibration of this model results (for more details see Gent et al., 2011; http://worldclim.com). The four scenarios are projected by the global climate model for four different representative concentration pathways (RCP) with a spatial resolution of 1 × 1 km (van Vuuren et al., 2011). The RCP each describe different climate scenarios that are regarded being possible depending on future amounts of greenhouse gas emissions, land use change and air pollutants, covering a wide range of scenarios presented in the existing literature. They incorporate various different technological, political, social and economic futures influencing climate change. Each RCP has been developed under the usage of a different model. For RCP2.6, greenhouse gas emissions are assumed to be very low, for RCP4.5 medium-low, for RCP6.0 medium, and RCP8.5 is seen as high emission scenario. Air pollution is assumed to be medium-low for RCP2.6, medium for RCP4.5 and RCP6.0, and medium-high for RCP8.5. Data were harmonized, downscaled or converted using e. g. a carbon-cycle climate model or atmospheric chemistry model for emission data to be transformed into concentration data (for more details see van Vuuren et al., 2011).

The data sets for organic C content, gravel content and bulk density were obtained from the WISE30sec data set available at http://isric.org with a spatial resolution of 1 × 1 km up to a depth of 2 m (for basic statistics on the soil properties see Table 2). The WISE30sec data set was compiled from different sources, such as the Harmonized World Soil Database, version 1.21 with marginal corrections, a climate zones map (Köppen-Geiger) used as co-variate and soil property estimations based on the ISRIC-WISE soil profile database. Soil properties were estimated based on statistical analyses of about 21,000 soil profiles. This was undertaken using an elaborate system of taxonomy-based transfer rules combined with expert-rules, which assess the consistency of the predictions within the pedons. These rules implemented in the derivations were marked to support in indicating the possible confidence in the estimated data regarding their lineage. WISE30sec is generally regarded as being appropriate for exploratory assessments at a resolution of 1 × 1 km (for more detailed information see Batjes, 2015).

The data to determine the spatial extension of the permafrost zone of the Qinghai-Tibet Plateau were obtained from the Global Permafrost Zonation Index Map available at http://www.geo.uzh.ch with a spatial resolution of 1 × 1 km. The model underlying this map is based on established relationships between air temperature and occurring permafrost, which have been transformed into this model. Its parametrization has been undertaken based on published approximations. Air temperature and elevation represent the input parameters for the model. The input data to derive the modeled spatial permafrost extension are based on various climatic and physical-geographic data sets such as the CRU TS 2.0, NCEP30 and SRTM30. Permafrost extension classes used in the data are: continuous permafrost (90–100%), extensive discontinuous permafrost (50–90%), sporadic discontinuous permafrost (10–50%) and isolated patches (smaller than 10%) (for more details see Gruber, 2012). In our study, continuous and extensive discontinuous permafrost are considered.

Table 2
Statistics of organic carbon content [g C kg^{-1}], bulk density [kg dm^{-3}] and coarse fragments (>2 mm) [vol.%] of the continuous and extensive discontinuous permafrost area on the Qinghai-Tibet Plateau based on WISE30sec data sets (Batjes, 2015).

Soil property	Organic carbon content [g C kg^{-1}]	Bulk density [kg dm^{-3}]	Coarse fragments (>2 mm) [vol.%]
Mean	31.03	1.25	14.34
Min	2.42	0.14	1
Max	425.23	1.62	46
Range	422.81	1.48	45
SD	42.26	0.19	6.88

2.3. Calculation of potential CO_2 emissions

The calculation of potential CO_2 emissions consists of two compartments: (i) General CO_2 emission rates for the Qinghai-Tibet Plateau as rather general soil respiration and (ii) specific CO_2 emission rates, i.e. thawing-induced CO_2 emissions, that focus on the additional source of C made available by climate change through permafrost thaw on the Qinghai-Tibet Plateau.

General CO_2 emission rates (i) as general soil respiration were calculated based on MAP for each scenario in 2050 and 2070 and the current situation using the regression model by Raich and Schlesinger (1992):

$$SR = 0.391P + 155 \quad (1)$$

where SR is the annual soil respiration rate (g C/m^2/yr) and P represents MAP (mm). This regression model performs best for estimating soil respiration on the Qinghai-Tibet Plateau according to a comparison of different regression models by Bosch et al. (2016).

As global model, however, this regression model does not consider the situation of the Qinghai-Tibet Plateau specifically concerning thawing permafrost under global warming, inhering a further source of CO_2 evolving from the soil. We therefore estimated these particular thawing-induced CO_2 emissions (ii) additionally based on estimates from a synthesis of incubation experiments with soil samples from the arctic region by Schädel et al. (2014). On average, 23.1% of the organic C can potentially be lost within 50 incubation years through permafrost thawing (Schädel et al., 2014), which corresponds to approximately 0.012‰ per day on average. With 166 frost-free days per year on the Qinghai-Tibet Plateau as average from 1960 to 2000 and approximately additional 3 days per further decade because of global warming (Zhang et al., 2014), the potential C loss from thawing permafrost C stocks is hence 0.222% on average per year from 2015 to 2050 and from 2015 to 2070 on average 0.226% per year. Accordingly, the potential organic C loss from 2015 to 2050 amounts to 7.78% and to 12.45% until 2070 of the organic C stock in 2015. As the amount of released CO_2 in the process of permafrost thaw is rather independent from the exact temperature (Schädel et al., 2014), a further differentiation according to the RCPs used in this study would not yield deeper insights.

C stocks for k layers as prerequsite for a calculation of thawing-induced soil CO_2 emissions were estimated as follows:

$$T_d = \sum_{i=1}^{k} \rho_i P_i D_i (1 - S_i), \quad (2)$$

where T_d represents the total amount of organic carbon (Mg m^{-2}) over depth d, ρ_i is bulk density (Mg m^{-3}) of the layer i, P_i equals the proportion of organic carbon in layer i (g C g^{-1}), D_i is the thickness of this layer (m), and S_i is the volume of coarse fragments (>2 mm) (Batjes, 1996).

With the potential C loss from current C stocks, the amount of the CO_2 equivalent as potential greenhouse gas emissions from the process of permafrost thaw for 2050 and 2070 can be calculated. This potential CO_2 emission rate is added to the CO_2 emission rates that were calculated for each scenario of 2050 and 2070 based on MAP for obtaining total CO_2 emissions. The proportion of thawing-induced CO_2 emissions to total CO_2 emissions was obtained as ratio for each year. To calculate this, means of total CO_2 emissions of all scenarios were averaged for each year.

3. Results

3.1. CO_2 emission scenarios for 2050

The four scenarios for 2050 project total CO_2 emissions ranging from lowest 1420.22 g CO_2 m^{-2} y^{-1} (RCP2.6) to highest 1433.46 g CO_2 m^{-2} y^{-1} on average (RCP8.5) (see Table 3). The difference between the lowest and highest mean CO_2 emission rate is hence 9.23‰. Differences in the minima and maxima of the different scenarios are likewise similar ranging from 737.90 g CO_2 m^{-2} y^{-1} (RCP4.5) to 739.13 g CO_2 m^{-2} y^{-1} (RCP8.5) (minima) and between 4188.95 g CO_2 m^{-2} y^{-1} (RCP2.6) and 4224.77 g CO_2 m^{-2} y^{-1} (RCP8.5) (maxima). The mean of the thawing-induced CO_2 emissions adds up to 36.47% of the averaged means of the total CO_2 emissions. In all scenarios, more values exceed the respective averages as reflected by the median values from 1254.03 g CO_2 m^{-2} y^{-1} (RCP6.0) to 1267.53 y^{-1} (RCP8.5). The frequency distribution of all thawing induced values differs strongly from those of the total CO_2 emissions, that is to say their medians amount to less than half of the mean. Highest decreases in total CO_2 emissions compared to the total CO_2 emissions in 2015 are located in the central part of the plateau (Fig. 3).

With regard to the abundance of CO_2 emission values for CO_2 emission classes, most values (69.13%–69.90%) occur in the low class (>0–916.05 g CO_2 m^{-2} y^{-1}) throughout all scenarios (see Table 4). In the highest class (>3664.21 g CO_2 m^{-2} y^{-1}), only <1‰ of the values appears, which corresponds to an area of 976–979 m^2. Differences between the scenarios show to be small (Fig. 2) amounting to <1% for all scenarios in all CO_2 emission classes. It has to be considered, however, in terms of area, that the difference between RCP2.6 and RCP8.5 is up to 10,865 m^2 in the lowest class and up to 7853 m^2 in the low class as examples. In this case, the CO_2 input to the atmosphere from more than 10,000 m^2 of the permafrost soils of the Qinghai-Tibet Plateau would be instead of 0–916.05 g CO_2 m^{-2} at least >916.05–1832.10 g CO_2 m^{-2} or even >1832.10–3664.21 g CO_2 m^{-2} within one year, which is two to four times more.

3.2. CO_2 emission scenarios for 2070

Mean CO_2 emissions of all scenarios for 2070 range from lowest 1409.73 g CO_2 m^{-2} y^{-1} (RCP2.6) to 1426.25 g CO_2 m^{-2} y^{-1} (RCP8.5). The strongest difference between two scenarios therefore remains 1.15%. Like for the scenarios in 2050, minima (733.97 − 738.32 g CO_2 m^{-2} y^{-1}) and maxima (4129.10–4158.69 g CO_2 m^{-2} y^{-1}) are also very close. Median values lie about 150 g CO_2 m^{-2} y^{-1} below averages (1245.85–1263.96 g CO_2 m^{-2} y^{-1}). For all scenarios, CO_2 emissions appear to be less than the CO_2 emissions of 2050. Again, as for the projections of 2050, the statistical means of the general soil respiration follows the same patterns corresponding to the one´s of the total CO_2 emissions. The mean of the thawing-induced CO_2 emissions adds up to 36.03% of the averaged means of the total CO_2 emissions. Like for 2050, the medians of the thawing-induced values amount to less than half of the mean. For all scenarios, the range of the thawing-induced values appears to be broader than the range of the general soil respiration, which is also true for the projections of 2050. Like for 2050, strongest decreases in total CO_2 emissions compared to the total CO_2 emissions in 2015 are located in the central part of the plateau (Fig. 3).

Basic patterns of the abundance of total CO_2 emissions of 2050 and 2070 in their respective classes resemble each other strongly. Most values occur in the low class (69.00–69.33%) and in the class for high CO_2 emission rates, again <1‰ is found. Differences between the scenarios follow the structures of the values´ distribution for 2050. Except for the entire lowest class and the medium class for the RCP8.5 scenario, more value of CO_2 emissions can generally be found in all scenarios of 2050. This corresponds to the result of general higher total CO_2 emissions in 2050. The highest difference between years and scenarios within one class amounts to 1.29% at the most.

3.3. C stocks

In the permafrost soils of the Qinghai-Tibet Plateau, on average, 67.00 kg C m^{-2} for 2015, 61.79 kg C m^{-2} and 58.66 kg C m^{-2} for 2050 and 2070 are stored according to our estimations based on the WISE30sec data set (see Table 5). Minima range from 5.88 kg C m^{-2} (2070) to 6.72 kg C m^{-2} (2015) and maxima from 338.92 kg C m^{-2} (2070) to 387.13 kg C m^{-2} (2015). Highest C stocks occur in the central part of the plateau (Fig. 4). For the permafrost-affected area of the Qinghai-Tibet Plateau, C stocks in 2015 add up to 68.59 Pg and to 63.25 Pg and 60.05 Pg for 2050 and 2070 respectively. The climate change-induced increase of microbial activity releases 5.42 Pg C from these permafrost soils between 2015 and 2050 and 8.54 Pg C between 2015 and 2070. The consequent decrease of C stocks is highest on the central part of the plateau for both 2050 and 2070 (Fig. 5).

Table 3
Statistics of potential CO_2 emissions: total CO_2 emissions, consisting of general soil respiration (I) and thawing-induced CO_2 emission (II) in g CO_2 m^{-2} y^{-1} [g C m^{-2} y^{-1}].

Year	Scenario	Type of CO_2 emission	Mean	Min	Max	Median	Range
			g CO_2 m^{-2} y^{-1} [g C m^{-2} y^{-1}]				
2050	RCP2.6	Total I	1420.22 [387.59]	739.02 [201.68]	4188.95 [1143.20]	1255.98 [342.77]	3449.92 [941.51]
			901.02 [245.90]	618.59 [168.82]	2418.89 [660.14]	855.15 [233.38]	1800.30 [491.32]
	RCP4.5	Total I	1423.87 [388.58]	737.90 [201.38]	4190.54 [1143.64]	1260.37 [343.96]	3452.64 [942.26]
			904.80 [246.93]	617.49 [168.52]	2412.00 [658.26]	860.21 [234.76]	1794.51 [489.74]
	RCP6.0	Total I	1421.76 [388.01]	738.62 [201.57]	4195.69 [1145.04]	1254.03 [342.23]	3457.06 [943.46]
			902.75 [246.37]	618.18 [168.71]	2374.59 [648.05]	855.26 [233.41]	1756.40 [479.34]
	RCP8.5	Total I	1433.46 [391.20]	739.13 [201.71]	4224.77 [1152.98]	1267.53 [345.92]	3485.63 [951.26]
			914.34 [249.54]	622.36 [169.85]	2349.27 [641.14]	859.62 [236.60]	1726.91 [471.29]
2070	RCP2.6	Total I	1409.73 [384.73]	735.46 [200.71]	4149.22 [1132.36]	1245.85 [340.00]	3413.76 [931.65]
			900.00 [245.62]	617.23 [168.45]	2423.50 [661.40]	755.633 [206.22]	1806.27 [492.95]
	RCP4.5	Total I	1414.14 [385.93]	733.97 [200.30]	4143.43 [1130.78]	1249.51 [341.00]	3409.45 [930.47]
			904.62 [246.88]	615.73 [168.04]	2485.10 [678.21]	757.06 [206.61]	1869.37 [510.17]
	RCP6.0	Total I	1414.88 [386.13]	736.89 [201.10]	4129.10 [1126.87]	1251.36 [341.51]	3392.20 [925.76]
			905.13 [247.02]	618.66 [168.84]	2354.76 [642.64]	757.06 [206.61]	1736.10 [473.8]
	RCP8.5	Total I	1426.25 [389.24]	738.32 [201.49]	4158.69 [1134.95]	1263.96 [344.94]	3420.37 [933.45]
			916.78 [250.18]	620.09 [169.23]	2435.97 [664.75]	765.63 [208.95]	1815.68 [495.52]
2015	Schädel et al. (2014)	II	529.91 [144.62]	53.20 [14.52]	3134.91 [855.55]	236.19 [64.46]	3008.31 [821.03]
2050	Schädel et al. (2014)	II	519.75 [141.84]	52.18 [14.24]	3002.82 [819.49]	231.69 [63.23]	2950.63 [805.25]
2070	Schädel et al. (2014)	II	510.30 [139.26]	51.23 [13.98]	2948.25 [804.60]	227.47 [62.08]	2897.01 [790.62]
2015	Bosch et al. (2016)	Total I	1415.59 [386.33]	737.08 [201.15]	4224.34 [1152.86]	1246.86 [340.28]	3487.25 [951.70]
			886.92 [242.05]	614.32 [167.73]	2340.46 [638.73]	863.83 [235.75]	1726.14 [471.08]

Table 4
Abundance of CO_2 emission values of per class of CO_2 emissions for the Qinghai-Tibet Plateau. CO_2 emission classes represent very low (>0–250 g C m^{-2} y^{-1}/>0–916.05 g CO_2 m^{-2} y^{-1}), low (>250–500 g C m^{-2} y^{-1}/>916.05–1832.10 g CO_2 m^{-2} y^{-1}), medium (>1832.10 g CO_2 m^{-2} y^{-1}–3664.21 g CO_2 m^{-2} y^{-1}/>500–1000 g C m^{-2} y^{-1}), high (>3664.21 g CO_2 m^{-2} y^{-1}/>1000 g C m^{-2} y^{-1}) and no (≤0 g CO_2 m^{-2} y^{-1}/≤0 g C m^{-2} y^{-1}] CO_2 emissions. Italicized values specify the area on the Qinghai-Tibet Plateau assigned to the respective CO_2 emission class.

Classes	Scenario	RCP2.6		RCP4.5		RCP6.0		RCP8.5	
	Year	2050	2070	2050	2070	2050	2070	2050	2070
		% [m^{-2}]							
Very low		13.27	13.50	13.29	13.50	12.72	13.06	12.21	12.99
		135,902	*138,276*	*136,118*	*138,286*	*130,224*	*133,737*	*125,037*	*132,997*
Low		69.25	69.18	69.13	69.00	69.74	69.57	69.90	69.33
		708,955	*708,160*	*707,685*	*709,400*	*713,895*	*712,163*	*715,538*	*709,707*
Medium		17.36	17.24	17.49	17.11	17.44	17.27	17.78	17.83
		177,789	*176,273*	*178,843*	*175,058*	*178,528*	*176,802*	*182,068*	*182,560*
High		0.09	0.08	0.09	0.08	0.09	0.08	0.09	0.09
		976	*912*	*976*	*878*	*977*	*920*	*979*	*969*
No		0.00	0.00	0.00	0.00	0.00	0.00	0.00	0.00
		0	*0*	*0*	*0*	*0*	*0*	*0*	*0*

4. Discussion

Overall, total CO_2 emissions for both 2050 and 2070 remain within the same order of magnitude of soil respiration generally measured on the Qinghai-Tibetan Plateau (2550.29 g CO_2 m^{-2} y^{-1} as average of four years) (Wang et al., 2014b) and further show a proportion of general soil respiration and thawing-induced CO_2 emissions comparably to the results of Peng et al. (2015) and Hicks Pries et al. (2013). The field measured results of Peng et al. (2015) with the amount of C additionally released due to warming and thawing permafrost, reach 18 to 29% in an alpine meadow on the plateau. In that study, there is no differentiation between altered soil CO_2 emissions induced by permafrost thaw and altered general soil CO_2 emissions due to a general higher plant and microbial metabolic activity as consequence of higher temperatures. However, it is to assume that most of the increase is related to the additional available permafrost C as Hicks Pries et al. (2013) obtained similar results when focusing on soil CO_2 emissions originating from permafrost C. In that study, old soil heterotrophic soil CO_2 emissions comprised up to approximately 18% of the remaining parts of soil CO_2 emissions under thawing permafrost.

The differences between the scenarios of total soil CO_2 emissions fully result from the differences between the general soil respiration rates for each scenario as the potential thawing-induced CO_2 emissions are represented by only one value per year due to their different calculation. Accordingly, values of mean, minimum, maximum and median share proportionally the same trends for total CO_2 emissions and general soil respiration. Differences between the scenarios of general soil CO_2 emissions appear to be about 1% what reflects the small differences between the scenarios of MAP as fully accounting for this.

The variability of the general soil respiration results from the variation in MAP, naturally not following static patterns as depending on complex influencing factors as partly considered in the RCPs. As the mean CO_2 emission rate of the RCP6.0 is lower than the one of the RCP4.5 in 2050, the CO_2 emission rate reflects that there is no general

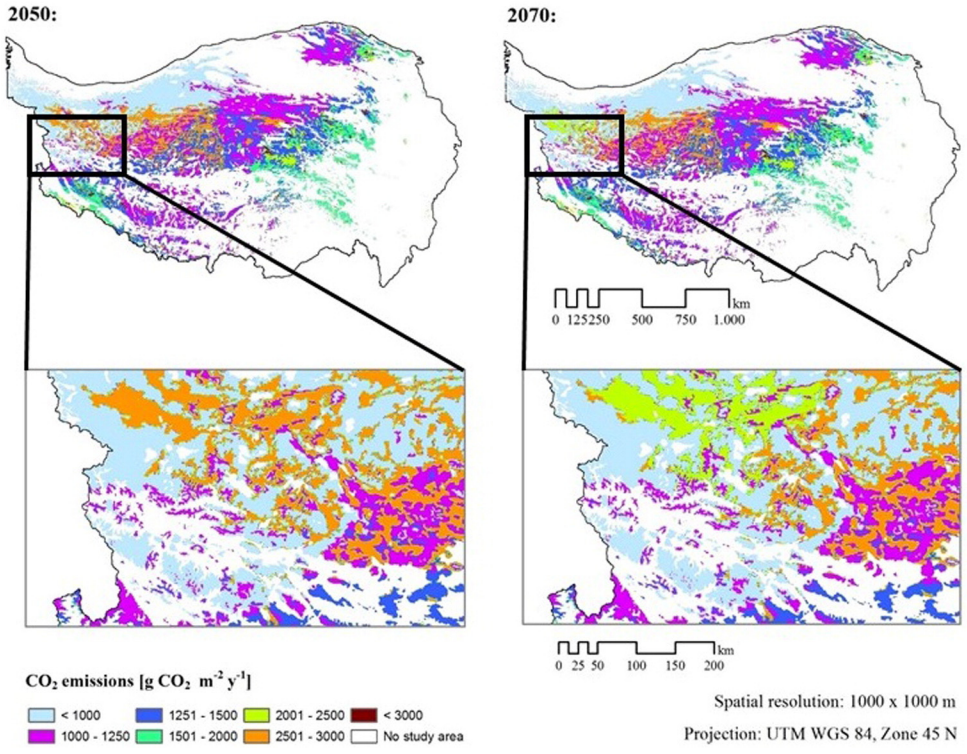

Fig. 2. Spatial distribution of total potential CO_2 emissions from permafrost-affected areas on the Qinghai-Tibet Plateau in 2050 and 2070 according to the RCP2.6 scenarios. Unit of CO_2 emissions is g CO_2 m^{-2} y^{-1}. The spatial resolution of the grids is 1000 × 1000 m.

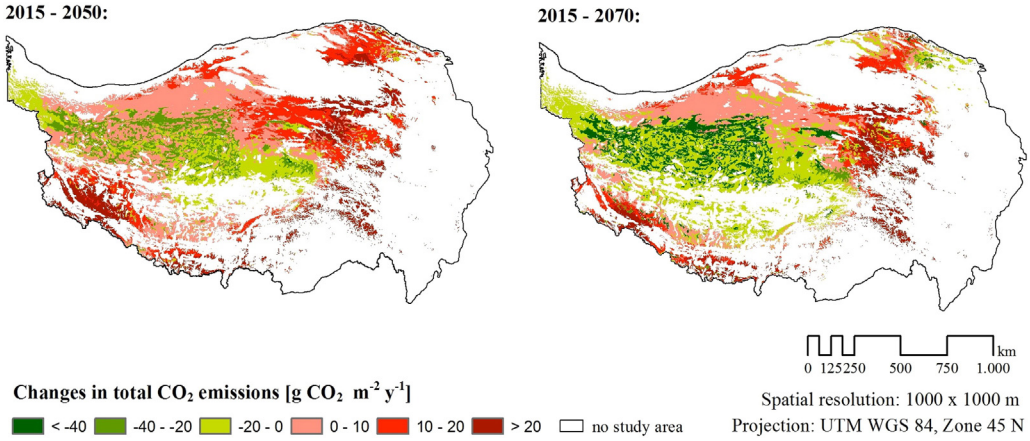

Fig. 3. Spatial distribution of absolute differences in total potential CO_2 emissions from permafrost-affected areas on the Qinghai-Tibet Plateau between 2015 and 2050 and between 2015 and 2070 according to the RCP2.6 scenarios. Unit of changes in total CO_2 emissions is g CO_2 m^{-2} y^{-1}. The spatial resolution of the grids is 1000 × 1000 m.

linear correlation to the radiative forcing values. For all scenarios of 2070, CO_2 emissions appear to be less than the CO_2 emissions of 2050. This results mostly from the thawing-induced CO_2 loss, which is calculated as percentage of the respective C-stock, consequently decreasing with temporal progression. Differences between the years 2050 and 2070 in thawing-induced CO_2 emissions reflect their linear calculation and decreasing C-stocks. As natural process, thawing of permafrost does, however, not progress strict linearily. Nevertheless, the relative high independence of temperature (Schädel et al., 2014) does not require further differentiations of different temperature scenarios.

Regarding the abundance of values in 2050, except for the entire lowest class and the medium class for the RCP8.5 scenario, more value of CO_2 emissions can generally be found in all scenarios of 2050. This corresponds to the result of general higher total CO_2 emissions in 2050, resulting from decreasing carbon stocks in the end.

With regard to the C stored in the permafrost soils of the Qinghai-Tibet Plateau, the decrease from 2015 to 2070 (Table 5) generally reflects the steady decrease caused by the raised C decomposition. The C stocks in general appear to be reasonable in view of other studies on C stocks. They fit the order of magnitude of field measured data with about 10 kg C m^{-2} in permafrost soils of alpine grasslands of the Qinghai-Tibet Plateau to a depth of <1 m (Genxu et al., 2008; Doerfer et al., 2013) or 56.5 kg C m^{-2} in meadows (Mu et al., 2015) as examples. The global C stock estimates by Batjes (2015) clearly show the same patterns of the spatial distribution of C stocks on the Qinghai-Tibet Plateau overall with highest C stocks on the Qinghai-Tibet Plateau reaching global maxima. Carvalhais et al. (2014) approximates the global maximum for soil C stocks to 243 kg C m^{-2}, which is comparable to the maxima in this study. Compared to 450 Pg C (Zimov et al., 2006) in the Siberian loess permafrost (1×10^6 km^2), the C stock estimated in this study appears to be much lower, resulting from the fact that it covers only a depth to 2 m in contrast to 25 m as reported in Zimov et al. (2006). They also include roots and partly organic matter in their less spatially differentiated approximations as not considering coarse fragments in their calculations and using only one standard value for organic C content and bulk density which accounts for much higher values. Their uncertainty is further assessed as possibly deviating by several hundred Pg (McGuire et al., 2010). Moreover, an extreme spatial variability of soil organic C stocks on the Qinghai-Tibet Plateau has been reported (Mu et al., 2015), leading generally to a wide range in area-wide estimations. C stocks for the permafrost region on the Qinghai-Tibet Plateau were calculated with about 160 Pg C up to 25 m in a similar order of magnitude by Mu et al. (2015) compared to the estimates for the Siberian loess permafrost. However, the strong methodological differences to this study are to a large extent very similar next to a broader definition of the permafrost area. Wang et al. (2002) estimate the C stock of the plateau´s grasslands to 33.5 Pg. However, they only consider the first 70 cm of the soil. The estimation of Mu et al. (2015) for the first two meters amount to about 27.9 Pg C for the permafrost soils on the Qinghai-Tibet Plateau indicating that estimates in this study are reasonable. Since the calculations by Mu et al. (2015) are based on literature data from different studies, they expect deviations of several 10% regarding the C contents as base for their calculations due to different methodological approaches.

With about 0.54 Pg CO_2 y^{-1}, the thawing-induced soil CO_2 emissions of the entire study area are, although in the same order of magnitude, about three times higher than what would be supposed based on the results of Schuur et al. (2009). They estimate 1 Pg C y^{-1} (3.66 Pg CO_2 y^{-1}) as global C flux assuming an estimated area of global permafrost with about $22 * 10^6$ km^2 according to Gruber (2012). Also, the estimates of Koven et al. (2011), who projected emissions from permafrost soils to a depth of 3 m to 7–17 Pg CO_2 until 2100, are lower than the results of this thesis (7.3.2). These and comparable estimates by Harden et al. (2012) are even considered being overestimated (Schädel et al., 2014). However, the results of Schuur et al. (2009) are highly uncertain since they are based on measurements on only one site. A recent, model-based study by Schuur et al. (2015) approximated 37–174 Pg C to lose from the global permafrost zone by 2100 under the RCP8.5 scenario. This corresponds to 0.09 Pg C y^{-1} from the plateau on average, which is distinctly closer to an average of 0.15 Pg C y^{-1} (Section 7.3.2). Generally, global annual soil CO_2 emissions are approximated to 63–120 Pg C (Raich and Schlesinger, 1992; Raich and Potter, 1995;

Table 5
Statistics of the soil C stocks of the Qinghai-Tibet Plateau in 2015, 2050 and 2070 in kg C m^{-2} up to a depth of 2 m.

Year	Mean	Min	Max	Median	Range	Sum [Pg C]	Sum of thawing-induced C loss since 2015 [Pg C]
	kg C m^{-2}						
2015	67.00	6.72	387.13	29.87	380.40	68.59	–
2050	61.79	6.20	356.98	27.54	350.78	63.25	5.34
2070	58.66	5.88	338.92	26.15	333.03	60.05	8.54

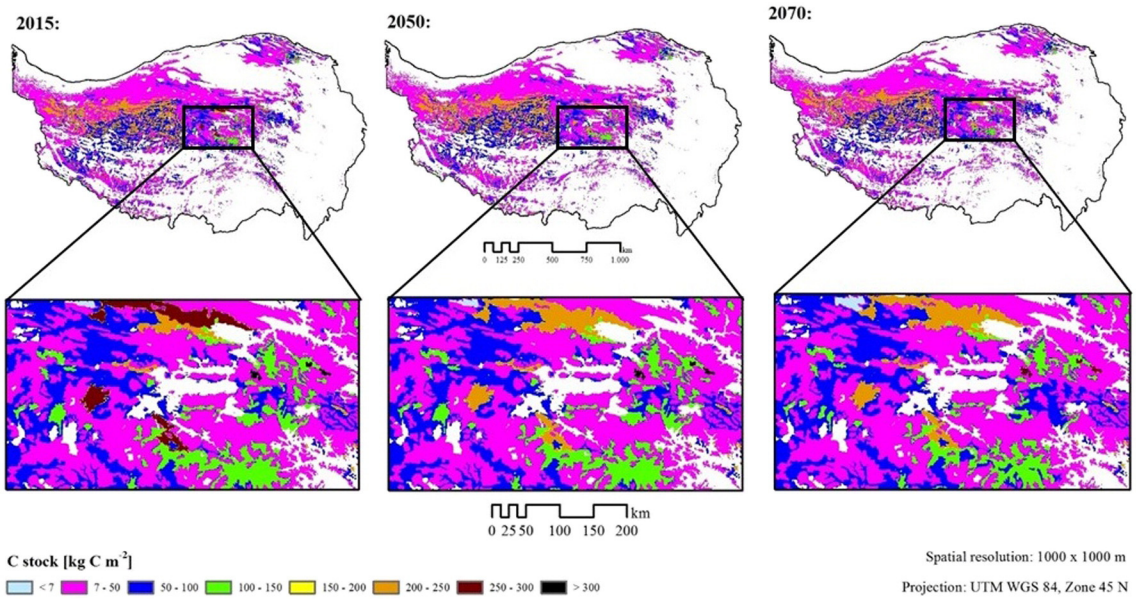

Fig. 4. Spatial distribution of C stocks of the permafrost-affected areas on the Qinghai-Tibet Plateau for 2015, 2050 and 2070. C stocks are in SI unit (kg m^{-2}). The spatial resolution of the grids is 1000 × 1000 m.

Reichstein and Beer, 2008). This gives rise to the assumption that the calculated heterotrophic soil CO_2 emissions induced by permafrost thaw are as a whole to be revised upwards after further research.

The spatial distribution of CO_2 emissions with a concentration of highest values in the central part of the plateau (Fig. 2) resembles the spatial distribution of the C:N ratio in the study area. There, the C:N ratio ranges from 0 to 25 (Batjes, 2015). Highest C losses occur in this area (Fig. 5), confirming the results of Schädel et al. (2014) that present the C:N ratio as most reliable predictor of C loss compared to either C or N concentration. The permafrost conditions, conserving fragmentary decomposed organic matter, may account for this positive relationship, which reflects the stabile presence of N in the system (Schädel et al., 2014).

Uncertainties of the presented potential CO_2 emissions result from various sources. Input data limitations restrict the estimations´ reliability in all cases. The WorldClim data sets generally show lower precision for poorly sampled regions like the Qinghai-Tibet Plateau (Maussion et al., 2011; Böhner, 2006; Hijmans et al., 2005). The same holds true for areas on the plateau with complex topography where a 1 × 1 km resolution does not capture all potential variation (Hijmans et al., 2005).

The projections of the global climate model Community Climate System Model Version 4 show uncertainties for precipitation on the Qinghai-Tibetan Plateau up to 10 mm per day compared to reference models. The RCP projections generally inhere deficiencies resulting from the process of harmonizing different scenarios and models underlying the RCPs (van Vuuren et al., 2011). As the years 2050 and 2070 represent an average from 2041 to 60 and 2061–80 respectively, likely variation is not represented. Assumptions are too general or static such as a general stronger and stronger regulation of air pollution (van Vuuren et al., 2011). They also may not only occur model-specifically but are important for other RCP such as reforestation policies included in RCP 4.5 but potentially also relevant to RCP 2.6. Further uncertainties arise from the transfer of emissions to concentrations and radiative forcing (van Vuuren et al., 2011). The RCP do not represent those various possible translations (van Vuuren et al., 2011). Moreover, the respective socio-economic scenario for each RCP is not representing the variety of possible developments (van Vuuren et al., 2011).

The data input sets from the WISE30sec data inhere deficiencies that arise from processing simplifications resulting in prediction accuracies from 23 to 51% (point-based). Potential biases occur especially for soil characteristics “not observed” as the volumetric gravel content that was calculated using taxotransfer rules. The pragmatic combination of soil profile data from different sources led in the process of harmonizing and reclassification to generalizations (Batjes, 2015). With different soil

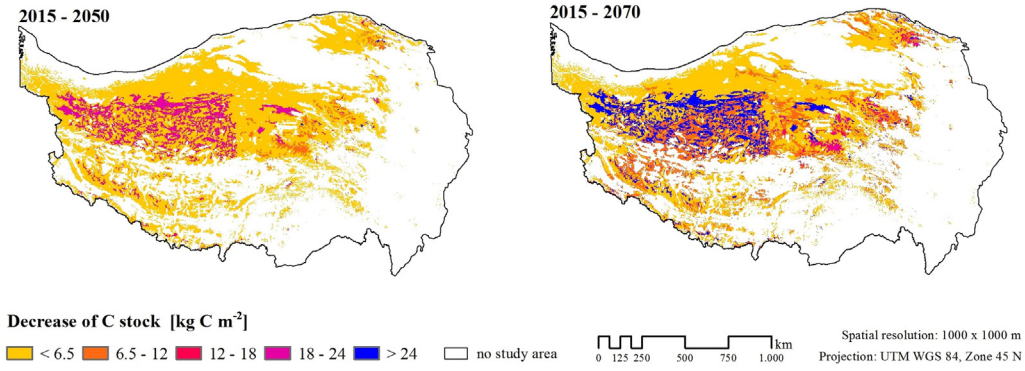

Fig. 5. Spatial distribution of absolute differences in C stocks of the permafrost-affected areas on the Qinghai-Tibet Plateau between 2015 and 2050 and between 2015 and 2070. Absolute differences in C stocks are in SI unit (kg m^{-2}). The spatial resolution of the grids is 1000 × 1000 m.

analytical methods in nearly each country, even possibly varying between laboratories, comparability remains critical. To some extend these differences result from the fact that the analytical procedures depend on the soil type. However, no straightforward method of harmonization of the data exists (Batjes, 1999), why the synthesis of the data has proceeded pragmatically as in studies before at this scale (Batjes, 2002). Also, soil geographic as well as taxonomic gaps do exist. Generally, the soil profiles are spatially irregularly distributed. Further uncertainties originating from the spatial data and processes of aggregation, are not yet possible to be quantified at present (Batjes, 2015). Despite their limitations, however, the WISE30sec data sets provide the most recent, appropriate, area-explicit information on soil properties for the Qinghai-Tibet Plateau needed to calculate C stocks at a resolution of 1 × 1 km to a depth of 2 m in order to assess potential soil CO_2 emissions on the Qinghai-Tibet Plateau.

In the Global Permafrost Zonation Index Map, main uncertainties also occur for less weakly researched areas like the Qinghai-Tibet Plateau (Gruber, 2012). Generally, the high spatial variability of permafrost is not captured by the resolution at hand. The occurrence of permafrost is a result of the interaction of various influencing factors. The Global Permafrost Zonation Index Map, however, solely determines the existence of permafrost based on mean annual air temperature leading to deficiencies. Excluding topographic effects such as the exposition of hills to sun or temperature effects of snow warming the underground are not represented. Likewise is deep permafrost not considered with its influence on near-surface conditions. The model on which the map is based on, further does not reproduce effects of valleys and depressions where inversions and the drainage of cold air often impact ground temperature. Vegetation effects and thermal characteristics of the ground are further not considered. Sub-grid variability may differ between grids which is also not reproduced by the map as well as transient effects (Gruber, 2012). Given the variety of definitions of permafrost, differences in the determination of the area covered by permafrost may occur (Gruber, 2012).

To sum up, using these freely accessible data inheres several limitations and uncertainties in general that have partly not even been quantified yet. Therefore, estimations based on them have to be used with caution in view of their deficiencies. In combining the different data sets with their respective limitations in data quality, the deficiencies become even more complex and less quantified. Also, the order of magnitude of potential deviations may change and results may not be as comparable e.g. absolute changes of general soil CO_2 emissions over time may range in a different order of magnitude than the changes over time of the thawing-induced soil CO_2 emissions in absolute numbers. In adding them up to total soil CO_2 emissions, this difference is less obvious and the results need to be interpreted carefully. However, on a regional scale as well as for exploratory investigations, the individual data sets are considered both appropriate and advantageous as highly efficient suppliers of area-explicit data at a high resolution. Their combination increases the inaccuracies of the results, why they as a matter of principle cannot reach the precision of using a fully consistent data set. This approach obtains its appropriateness in view of the early stage of this research area together with its relevance to the vital problem of climate change necessitating results in a timely manner, and other approaches still being highly uncertain as well.

With regard to the computation of the general soil respiration, limitations arise from the background of the regression model by Raich and Schlesinger (1992). Indicated by its coefficient of determination ($r^2 = 0.34$), it is not capable to fully explain the data variability reflecting highly complex interdependencies between soil respiration and all its controlling factors.

Next to this, high small-scale variability of CO_2 emission rates especially in alpine meadows is not captured by a data resolution of 1 × 1 km. The comparatively very high values in alpine meadows of especially the *Kobresia tibetica* plant communities cannot not be predicted with this spatial resolution. This strong difference in CO_2 emission rates between this communities and other alpine meadow plant communities results in wide differences of CO_2 emissions within short distances which can only be represented by a higher spatial resolution.

Moreover, the degradation of vegetation and grazing effects comprising about 35% of the Qinghai-Tibet Plateau with decreasing influence on soil respiration (Wen et al., 2013; Cao et al., 2004) is not integrated in our estimations and constraints these predictions of CO_2 emissions. Grazing influences permafrost thawing as decreasing vegetation cover reduces the insulating effect of vegetation, resulting in quicker permafrost thaw on the Qinghai-Tibet Plateau (Hu et al., 2009) and consequently to higher CO_2 emissions induced by permafrost thaw. Although the mechanisms of the relations have in general not been sufficiently clarified yet, changes in soil CO_2 emissions by grazing are relatively high with a decrease by about 50% when doubling grazing intensity on the Qinghai-Tibet Plateau (Cao et al., 2004). Moderate grazing reduces the C uptake in *Kobresia* turfs (Babel et al., 2014) indicating decreasing CO_2 emissions. Johnson and Matchett (2001) concluded that grazing resulted in a decrease of soil CO_2 emissions compared to an ungrazed tallgrass prairie, however, grazed prairie exhibited more soil CO_2 emissions than ungrazed prairie (Frank et al., 2002). Thus, although important, grazing effects do not exceed the order of magnitude of the remaining soil CO_2 emissions (Cao et al., 2004).

Another limitation of the potential thawing-induced CO_2 emissions in the presented results arise from the transfer of the incubation experiments as base for the calculations. The soil samples of the experiments originate from the Arctic with different climatic and environmental conditions. As the soil samples are taken from different studies, their sampling methods are not fully consistent inhering a potential source of uncertainty. Further, the thawing experiments are executed under laboratory conditions that may deviate from the process in natural environment due to strong simplifications. Fresh litter additionally incorporated into the soil is not regarded as well as it is assumed that abiotic factors do not change in contrast to a natural environment (Schädel et al., 2014). Of special importance are drainage conditions altering thawing-induced C loss by 9–75% (Elberling et al., 2013). Uncertainty further arises from the extrapolation of the results up to 50 years, disregarding potential variation over time. It is further to expect that the linear developement of C loss over time assumed for the calculations presented here does not correspond to the natural course as climate change is characterized by a high complexity.

Next to that limitation, we did not include areas with permafrost soils covering <50% of the area indicating that our estimates are possibly biased low. However, their inclusion would potentially have caused a stronger bias.

Moreover, the permafrost of the Qinghai-Tibet Plateau may reach a depth up to more than 130 m (Wang and French, 1995) and soil C stocks at least several 10 m (Mu et al., 2015). Consequently, the C stocks must be higher than the $WISE_{30sec}$ data set captures with a depth of 2 m. Thus, the thawing-induced CO_2 emissions in the field are higher, however, it is to assume that the permafrost thawing process does not reach this depth within the addressed years (Pang et al., 2012).

5. Conclusion

Estimates of potential CO_2 emissions from permafrost soils are crucial to understanding feedback mechanisms of global warming to project future scenarios of climate change. The magnitude of future CO_2 emissions is challenging to predict because of existing high uncertainties about quantity and velocity of the release of organic C from permafrost. Especially for the Qinghai-Tibet Plateau as key region, uncertainties in area-wide data are high as data collection requires extremely high time and cost efforts. Data at a sufficient spatial resolution for large areas, especially for the Qinghai-Tibet Plateau, are generally scarce.

Using different scenarios, a regression model that can be run with climate data, results from laboratory experiments with soil samples

from the northern circumpolar permafrost zone, and C stock estimations, we provide an area-wide, highly resoluted, first estimate of potential CO_2 emissions for 2050 and 2070 from permafrost soils of the Qinghai-Tibet Plateau, thus being advantageous for an area-wide calculation of stronger differentiated climate change scenarios.

From our estimates, we conclude that thawing-induced soil CO_2 emissions from permafrost soils on the Qinghai-Tibet Plateau increase general soil respiration by at least about one third, considering that an incorporation of deep permafrost carbon would further distinctly raise CO_2 emissions. Differences between scenarios remain <1% and thawing-induced CO_2 emissions generally decrease comparing 2015, 2050 and 2070. Our approach of aiming at a first estimate of CO_2 emissions of permafrost soils of the Qinghai-Tibet Plateau under climate change conditions is consistent to measurements of C loss from thawing permafrost soils measured within other studies. The spatially distinct CO_2 emissions calculation at a comparably high spatial resolution allows for assessing both an area-specific future permafrost carbon feedback to climate change from the highly vulnerable permafrost carbon of the Qinghai-Tibet Plateau and spatially distinct future potential greenhouse gas emissions.

Acknowledgements

We thank the Evangelisches Studienwerk Villigst e. V. that funded this study conducted within the framework of the research project PERMATRANS. The support by the German Federal Ministry for Education and Research (BMBF, grant no. 03G0810A) is highly acknowledged. We further appreciate very much the assisstance with data processing of Sarah Schönbrodt-Stitt (University of Tuebingen).

References

Amundson, R., 2001. The carbon budget in soils. Annu. Rev. Earth Planet. Sci. 29, 535–562.
Babel, W., Biermann, T., Coners, H., Falge, E., Seeber, E., Ingrisch, J., Schleuß, P.-M., Gerken, T., Leonbacher, J., Leipold, T., Willinghöfer, S., Schützenmeister, K., Shibistova, O., Becker, L., Hafner, S., Spielvogel, S., Li, X., Xu, X., Sun, Y., Zhang, L., Yang, Y., Ma, Y., Wesche, K., Graf, H.-F., Leuschner, C., Guggenberger, G., Kuzyakov, Y., Miehe, G., Foken, 2014. Pasture degradation modifies the water and carbon cycles of the Tibetan highlands. Biogeosciences 11, 6633–6656.
Batjes, N.H., 1996. Total carbon and nitrogen in the soils of the world. Eur. J. Soil Sci. 47, 151–163.
Batjes, N.H., 1999. Soil vulnerability mapping in Central and Eastern Europe: issues of data acquisition, quality control and sharing. In: Naff, T. (Ed.), Data Sharing for International Water Resource Management: Eastern Europe, Russia and the CIS. NATO Science Series 2: Environmental Security (Vol. 61). Kluwer Academic Publishers, Dordrecht, pp. 187–206.
Batjes, N.H., 2002. Soil parameter estimates for the soil types of the world for use in global and regional modelling (Version 2.1). ISRIC Report 2002/02c, International Food Policy Research Institute (IFPRI) and International Soil Reference and Information Centre (ISRIC), Wageningen Available at: http://www.isric.org/isric/webdocs/Docs/ISRIC_Report_2002_02c.pdf; (accessed 12/2008., 58 p).
Batjes, N.H., 2015. World soil property estimates for broad-scale modelling (WISE30sec). Report 2015/01. ISRIC – World Soil Information, Wageningen.
Baumann, F., He, J.-S., Schmidt, K., Kühn, P., Scholten, T., 2009. Pedogenesis, permafrost, and soil moisture as controlling factors for soil nitrogen and carbon contents across the Tibetan Plateau. Glob. Chang. Biol. 15, 3001–3017.
Baumann, F., Schmidt, K., Doerfer, C., He, J.-S., Scholten, T., Kühn, P., 2014. Pedogenesis, permafrost, substrate and topography: plot and landscape scale interrelations of weathering processes on the central-eastern Tibetan Plateau. Geoderma 226-227, 300–316.
Böhner, J., 2006. General climatic controls and topoclimatic variations in Central and High Asia. Boreas 35, 279–295.
Böhner, J., Lehmkuhl, F., 2005. Environmental change modelling for Central and High Asia: Pleistocene, present and future scenarios. Boreas 34, 220–231.
Bond-Lamberty, B., Thomson, A., 2010a. Temperature-associated increases in the global soil respiration record. Nature 464, 579–582.
Bond-Lamberty, B., Thomson, A., 2010b. A global database of soil respiration data. Biogeosciences 7, 1915–1926.
Bosch, A., Doerfer, C., He, J.-S., Schmidt, K., Scholten, T., 2016. Predicting soil respiration for the Qinghai-Tibet Plateau: an empirical comparison of regression models. Pedobiologia 59, 41–49.
Cao, G., Tang, Y., Mo, W., Wang, Y., Li, Y., Zhao, X., 2004. Grazing intensity alters soil respiration in an alpine meadow on the Tibetan plateau. Soil Biol. Biochem. 36, 237–243.
Carvalhais, N., Forkel, M., Khomik, M., Bellarby, J., Jung, M., Migliavacca, M., Mu, M., Saatchi, S., Santoro, S., Santoro, M., Thurner, M., Weber, U., Ahrens, B., Beer, C., Cescatti, A., Randerson, J.T., Reichstein, M., 2014. Global covariation of carbon turnover times with climate in terrestrial ecosystems. Nature 514, 213–217.
Chapin III, F.S., Sturm, M., Serreze, M.C., McFadden, J.P., Key, J.R., Lloyd, A.H., McGuire, A.D., Rupp, T.S., Lynch, A.H., Schimel, J.P., Beringer, J., Chapman, W.L., Epstein, H.E., Euskirchen, E.S., Hinzman, L.D., Jia, G., Ping, C.-L., Tape, K.D., Thompson, C.D.C., Walker, D.A., Welker, J.M., 2005. Role of land-surface changes in Arctic summer warming. Science 310, 657–660.
Chen, X., Post, W., Norby, R., Classen, A., 2010. Modeling soil respiration and variations in source components using a multi-factor global climate change experiment. Clim. Chang. 1–22.
Cheng, G., 2005. Permafrost studies in the Qinghai-Tibet Plateau for road construction. J. Cold Reg. Eng. 19, 19–29.
Cheng, G., Jin, H., 2013. Permafrost and groundwater on the Qinghai-Tibet Plateau and in northeast China. Hydrogeol. J. 21, 5–23.
Christensen, J.H., Hewitson, B., Busuioc, A., Chen, A., Gao, X., Held, I., Jones, R., Kolli, R.K., Kwon, W.T., Laprise, R., Rueda, V.M., Mearns, L., Menéndez, C.G., Räisänen, J., Rinke, A., Sarr, A., Whetton, P., 2007. Regional climate projections. In: Solomon, S., Qin, D., Manning, M., Chen, Z., Marquis, M., Averyt, K.B., Tignor, M., Miller, H.L. (Eds.), Climate Change 2007: The Physical Science Basis. Contribution of Working Group I to the Fourth Assessment Report of the Intergovernmental Panel on Climate Change. Cambridge University Press, Cambridge, pp. 848–940.
Davidson, E.A., Janssens, I.A., 2006. Temperature sensitivity of soil carbon decomposition and feedbacks to climate change. Nature 440, 165–173.
Ding, J., Li, F., Yang, G., Chen, L., Zhang, B., Liu, L., Fang, K., Qin, S., Chen, Y., Peng, Y., Ji, C., He, H., Smith, P., Yang, Y., 2016. The permafrost carbon inventory on the Tibetan Plateau: a new evaluation using deep sediment cores. Glob. Chang. Biol. http://dx.doi.org/10.1111/gcb.13257.
Doerfer, C., Kuehn, P., Baumann, F., He, J.-S., Scholten, T., 2013. Soil organic carbon pools and stocks in permafrost-affected soils on the Tibetan Plateau. PLoS One 8 (2), e57024.
Duan, A.M., Wu, G.X., 2005. Role of the Tibetan Plateau thermal forcing in the summer climate patterns over subtropical Asia. Clim. Dyn. 24, 793–807.
Dutta, K., Schurr, E.A.G., Neff, J.C., Zimov, S.A., 2006. Potential carbon release from permafrost soils of Northeastern Siberia. Glob. Change Biol. 12, 2336–2351.
Elberling, B., Michelsen, A., Schädel, C., Schuur, E.A.G., Christiansen, H.H., Berg, L., Tamstorf, M.P., Sigsgaard, C., 2013. Long-term CO_2 production following permafrost thaw. Nat. Clim. Chang. 3, 890–894.
Fan, J.-W., Shao, Q.-Q., Liu, J.-Y., Wang, J.-B., Harris, W., Chen, Z.-Q., Zhong, H.-P., Xu, X.-L., Liu, R.-G., 2010. Assessment of effects of climate change and grazing activity on grassland yield in the Three Rivers Headwaters Region of Qinghai-Tibet Plateau. China. Environ. Monit. Assess. 170, 571–584.
Frank, A.B., Liebig, M.A., Hanson, J.D., 2002. Soil carbon dioxide fluxes in northern semiarid grasslands. Soil Biol. Biochem. 34, 1235–1241.
Geng, Y., Wang, Y., Yang, K., Wang, S., Zeng, H., Baumann, F., Kuehn, P., Scholten, T., He, J.-S., 2012. Soil respiration in Tibetan alpine grasslands: belowground biomass and soil moisture, but not soil temperature, best explain the large-scale patterns. PLoS One 7, 1–12.
Gent, P.R., Danabasoglu, G., Donner, L.J., Holland, M.M., Hunke, E.C., Jayne, S.R., Lawrence, D.M., Neale, R.B., Rasch, P.J., Vertenstein, M., Worley, P.H., Yang, Z.-L., Zhang, M., 2011. The community climate system model version 4. J. Clim. 24, 4973–4991.
Genxu, W., Yuanshou, L., Yibo, W., Qingbo, W., 2008. Effects of permafrost thawing on vegetation and soil carbon pool losses on the Qinghai. Tibet Plateau, China, Geoderma 143, 143–152.
Gruber, S., 2012. Derivation and analysis of a high-resolution estimate of global permafrost zonation. Cryosphere 6, 221–233.
Harden, J.W., Sundquist, E.T., Stallard, R.F., Mark, R.K., 1992. Dynamics of soil carbon during deglaciation of the Laurentide Ice Sheet. Sciene 258, 1921–1924.
Harden, J.W., Koven, C.D., Ping, C.L., Hugelius, G., McGuire, A.D., Camill, P., Jorgenson, T., Kuhry, P., Michaelson, G.J., O´Donell, J.A., Schuur, E.A.G., Tarnocai, C., Johnson, K., Grosse, G., 2012. Field information links permafrost carbon to physical vulnerabilities of thawing. Geophys. Res. Lett. 39, L15704.
Hicks Pries, C.E., Schuur, E.A.G., Crummer, K.G., 2012. Holocene carbon stocks and carbon accumulation rates altered in soils undergoing permafrost thaw. Ecosystems 15, 162–173.
Hicks Pries, C., Schuur, E.A.G., Crummer, K.G., 2013. Thawing permafrost increases old soil and autotrophic respiration in tundra: partitioning ecosystem respiration using $\delta^{13}C$ and $\Delta^{14}C$. Glob. Change Biol. 19, 649–661.
Hijmans, R.J., Cameron, S.E., Parra, J.L., Jones, P.G., Jarvis, A., 2005. Very high resolution interpolated climate surfaces for global land areas. Int. J. Climat. 25, 1965–1978.
Hu, H., Wang, G., Liu, G., Li, T., Ren, D., Wang, Y., Cheng, H., Wang, J., 2009. Influences of alpine ecosystem degradation on soil temperature in the freezing-thawing process on Qinghai–Tibet Plateau. Environ. Geol. 57, 1391–1397.
Immerzeel, W., Quiroz, R., Jong, S., 2005. Understanding precipitation patterns and land use interaction in Tibet using harmonic analysis of SPOT VGT-S10 NDVI time series. Int. J. Remote Sens. 26, 2281–2296.
Jia, B., Zhou, G., Wang, Y., Wang, F., Wang, X., 2006. Effects of temperature and soil water-content on soil respiration of grazed and ungrazed *Leymus chinensis* steppes. Inner Mongolia. J. Arid Environ. 67, 60–76.
Johnson, L.C., Matchett, J.R., 2001. Fire and grazing regulate belowground processes in a tallgrass prairie. Ecology 82, 3377–3389.
Jones, C.D., Cox, P.M., Essery, R.L.H., Roberts, D.L., Woodage, M.J., 2003. Strong carbon cycle feedbacks in a climate model with interactive CO_2 and sulphate aerosols. Geophys. Res. Lett. 30, 1–4.
Kang, S., Xu, Y., You, Q., Flügel, W.-A., Pepin, N., Yao, T., 2010. Review of climate and cryospheric change in the Tibetan Plateau. Environ. Res. Lett. 5, 1–8.
Kirschbaum, M.U.F., 1995. The temperature dependence of soil organic matter decomposition, and the effect of global warming on soil organic storage. Soil Biol. Biochem. 27, 753–760.

Koven, C.D., Ringeval, B., Friedlingstein, P., Ciais, P., Cadule, P., Khvorostyanov, D., Krinner, G., Tarnocai, C., 2011. Permafrost carbon-climate feedbacks accelerate global warming. Proc. Natl. Acad. Sci. U. S. A. 108, 14769–14774.
Kutzbach, J.E., Liu, X., Liu, Z., Chen, G., 2008. Simulation of the evolutionary response of global summer monsoons to orbital forcing over the past 280,000 years. Clim. Dyn. 30, 567–579.
Lawrence, D.M., Koven, C.D., Swenson, S.C., Riley, W.J., Slater, A.G., 2015. Permafrost thaw and resulting soil moisture changes regulate projected high-latitude CO_2 and CH_4 emissions. Environ. Res. Lett. 10, 1–11.
Liu, X., Chen, B., 2000. Climatic warming in the Tibetan Plateau during recent decades. Int. J. Climat. 20, 1729–1742.
Luo, T., Li, W., Zhu, H., 2002. Estimated biomass and productivity of natural vegetation on the Tibetan Plateau. Ecol. Appl. 12, 980–997.
Manabe, S., Terpstra, T., 1974. The effects of mountains on the general circulation of the atmosphere as identified by numerical experiments. J. Atmos. Sci. 31, 3–42.
Maussion, F., Scherer, D., Finkelnburg, R., Richter, J., Yang, W., Yao, T., 2011. WRF simulation of a precipitation event over the Tibetan Plateau, China – an assessment using remote sensing and ground observations. Hydrol. Earth Syst. Sci. 15, 1795–1817.
McGuire, A.D., Macdonals, R.W., Schuur, E.A.G., Harden, J., Kuhry, P., Hayes, D.J., Christensen, T.R., Heimann, M., 2010. The carbon budget of the northern cryosphere region. Curr. Opin. Environ. Sustain. 2, 231–236.
Mu, C., Zhang, T., Wu, Q., Peng, X., Cao, B., Zhang, X., Cao, B., Cheng, G., 2015. Editorial: organic carbon pools in permafrost regions on the Qinghai-Xizang (Tibetan) Plateau. Cryosphere 9, 479–486.
Pang, Q., Zhao, L., Li, S., Ding, Y., 2012. Active layer thickness variations on the Qinghai-Tibet Plateau under the scenarios of climate change. Environ. Earth Sci. 66, 849–857.
Pei, Z.-Y., Ouyang, H., Zhou, C.-P., Xu, X.-L., 2009. Carbon balance in an alpine steppe in the Qinghai-Tibet Plateau. J. Integr. Plant Biol. 51, 521–526.
Peng, F., Xue, X., You, Q., Zhou, X., Wang, T., 2015. Warming effects on carbon release in a permafrost area of Qinghai-Tibet Plateau. Environ. Earth Sci. 73, 57–66.
Raich, J.W., Potter, C.S., 1995. Global patterns of carbon dioxide emissions from soils. Glob. Biogeochem. Cycles 9, 23–36.
Raich, J.W., Schlesinger, W.H., 1992. The global carbon dioxide flux in soil respiration and its relationship to vegetation and climate. Tellus 44B, 81–99.
Reichstein, M., Beer, C., 2008. Soil respiration across scales: the importance of a model-data integration framework for data interpretation. J. Plant Nutr. Soil Sci. 171, 344–354.
Rodeghiero, M., Cescatti, A., 2005. Main determinants of forest soil respiration along an elevation/temperature gradient in the Italian Alps. Glob. Chang. Biol. 11, 1024–1041.
Rodeghiero, M., Churkina, G., Martinez, C., Scholten, T., Gianelle, D., Cescatti, A., 2013. Components of forest soil CO_2 efflux estimated from $\Delta^{14}C$ values of soil organic matter. Plant Soil 364 (1), 55–68.
Schädel, C., Schuur, E.A.G., Bracho, R., Elberling, B., Knoblauch, C., Lee, H., Luo, Y., Shaver, G.R., Turetsky, M.R., 2014. Circumpolar assessment of permafrost C quality and its vulnerability over time using long-term incubation data. Glob. Change Biol. 20, 641–652.
Schaefer, K., Zhang, T., Bruhwiler, L., Barrett, A.P., 2011. Amount and timing of permafrost carbon release in response to climate warming. Tellus 63B, 165–180.
Schlesinger, W.H., Andrews, J.A., 2000. Soil respiration and the global carbon cycle. Biogeochemistry 48, 7–20.
Schönbrodt-Stitt, S., Bosch, A., Behrens, T., Hartmann, H., Xuezheng, S., Scholten, T., 2013. Approximation and spatial regionalization of rainfall erosivity based on sparse data in a mountainous catchment of the Yangtze River in Central China. Environ. Sci. Pollut. Res. 20, 6917–6933.
Schroeder, P.E., Winjum, J.K., 1995. Assessing Brazil's carbon budget I. Biotic carbon pools. For. Ecol. Manag. 75, 77–86.
Schuur, E.A.G., Bockheim, J., Canadell, J.G., Euskirchen, E., Field, C.B., Goryachkin, S.V., Hagemann, S., Kuhry, P., Lafleur, P.M., Lee, H., Mazhitova, G., Nelson, F.E., Rinke, A., Romanovsky, V.E., Shiklomanov, N., Tarnocai, C., Venensky, S., Vogel, J., Zimov, S.A., 2008. Vulnerability of permafrost carbon to climate change: implications for the global carbon cycle. Bioscience 58, 710–714.
Schuur, E.A.G., Vogel, J.G., Crummer, K.G., Lee, H., Sickman, J.O., Osterkamp, T.E., 2009. The effect of permafrost thaw on old carbon release and net carbon exchange from tundra. Nature 459, 556–559.
Schuur, E.A.G., McGuire, A.D., Schädel, C., Grosse, G., Harden, J.W., Hayes, D.J., Hugelius, G., Koven, C.D., Kuhry, P., Lawrence, D.M., Natalo, S.M., Olefeldt, D., Romanovsky, V.E., Schaefer, K., Turetsky, M.R., Treat, C.C., Vonk, J.E., 2015. Climate change and the permafrost carbon feedback. Nature 520, 171–179.
Shaver, G.R., Canadell, J., Chapin III, F.S., Gurevitch, J., Harte, J., Henry, J., Inseon, P., Jonasson, S., Melillo, J., Pitelka, L., Rustad, L., 2000. Global warming and terrestrial ecosystems: a conceptual framework for analysis. Bioscience 50, 871–882.
Sistla, S.A., Moore, J.C., Simpson, R.T., Gough, L., Shaver, G.R., Schimel, J.P., 2013. Long-term warming restructures Arctic tundra without changing net soil carbon storage. Nature 497, 615–618.
Valentini, R., Matteucci, G., Dolman, A.J., Schulze, E.-D., Rebmann, C., Moors, E.J., Granier, A., Gross, P., Jensen, N.O., Pilegaard, K., Lindroth, A., Grelle, A., Bernhofer, C., Grünwald, T., Aubinet, M., Ceulemans, R., Kowalski, A.S., Vesala, T., Rannik, Ü., Berbigier, P., Loustau, D., Guðmundsson, J., Thorgeirsson, H., Ibrom, A., Morgenstern, K., Clement, R., Moncrieff, J., Montagnani, L., Minerbi, S., Jarvis, P.G., 2000. Respiration as the main determinant of carbon balance in European forests. Nature 404, 861–865.
van Vuuren, D.P., Edmonds, J., Kainuma, M., Riahi, K., Thomson, A., Hibbard, K., Hurtt, G.C., Kram, T., Krey, V., Nakicenovic, N., Smith, S.J., Rose, S.K., 2011. The representative concentration pathways: an overview. Clim. Chang. 109, 5–31.
Wang, B., French, H., 1995. Permafrost on the Tibet Plateau, China. Quat. Sci. Rev. 14, 225–274.
Wang, S., Jin, H., Li, S., Zhao, L., 2000. Permafrost degradation on the Qinghai-Tibet Plateau and its environmental impacts. Permafrost Periglacial Process. 11, 43–53.
Wang, W.Y., Wang, Q.J., Li, S.X., Wang, G., 2006. Distribution and species diversity of plant communities along transect on the Northeastern Tibetan plateau. Biodivers. Conserv. 15, 1811–1828.
Wang, B., Bao, Q., Hoskins, B., Wu, G., Liu, Y., 2008. Tibetan Plateau warming and precipitation change in East Asia. Geophys. Res. Lett. 35.
Wang, G., Qian, J., Cheng, G., Lai, Y., 2002. Soil organic carbon pool of grassland soil son the Qinghai-Tibetan Plateau and its global implication. Sci. Total Environ. 291, 207–217.
Wang, X., Liu, L., Piao, S., Janssens, I.A., Tang, J., Liu, W., Chi, Y., Wang, J., Xu, S., 2014a. Soil respiration under climate warming: differential response of heterotrophic and autotrophic respiration. Glob. Chang. Biol. 20, 3229–3237.
Wang, Y., Liu, H., Chung, H., Yu, L., Mi, Z., Geng, Y., Jing, X., Wang, S., Zeng, H., Cao, G., Zhao, X., He, J.-S., 2014b. Non-growing-season soil respiration is controlled by freezing and thawing processes in the summer monsoon-dominated Tibetan alpine grassland. Global Biochem. Cy. 28, 1081–1095.
Wen, L., Dong, S., Li, Y., Wang, X., Li, X., Shi, J., Dong, Q., 2013. The impact of land degradation on the C pools in alpine grasslands of the Qinghai-Tibet Plateau. Plant Soil 368, 329–340.
Xu, Z.X., Gong, T.L., Li, J.Y., 2008. Decadal trend of climate in the Tibetan Plateau - regional temperature and precipitation. Hydrol. Process. 22, 3056–3065.
Xue, K.M., Yuan, M.J., Shi, Z., Qin, Y., Deng, Y., Cheng, L., Wu, L., He, Z., Van Nostrand, J.D., Bracho, R., Natali, S., Schuur, E.A.G., Luo, C., Konstantinidis, K.T., Wang, Q., Cole, J.R., Tiedje, J.M., Luo, Y., Zhou, J., 2016. Tundra soil carbon is vulnerable to rapid microbial decomposition under climate warming. Nature Clim. Change (advance online publication).
Yang, M., Wang, S., Yao, T., Gou, X., Lu, A., Guo, X., 2004. Desertification and its relationship with permafrost degradation in Qinghai-Xizang (Tibet) plateau. Cold Reg. Sci. Technol. 39, 47–53.
Yang, Y., Fang, J., Smith, P., Tang, Y., Chen, A., Ji, C., Hu, H., Rao, S., Tan, K.U.N., He, J.-S., 2009. Changes in topsoil carbon stock in the Tibetan grasslands between the 1980s and 2004. Glob. Chang. Biol. 15, 2723–2729.
Yu, H.Y., Luedeling, E., Xu, J.C., 2010. Winter and spring warming result in delayed spring phenology on the Tibetan Plateau. Proc. Natl. Acad. Sci. U. S. A. 107, 22151–22156.
Zhang, Y., Bingyuan, L., Du, Z., 2002. The area and boundary of Qinghai-Tibet Plateau. Geogr. Res. 21, 1–8 in Chinese.
Zhang, Y., Ohata, T., Kodata, T., 2003. Land-surface hydrological processes in the permafrost region of the eastern Tibetan Plateau. J. Hydrol. 283, 41–56.
Zhang, Y., Tang, Y., Jiang, J., Yang, Y., 2007. Characterizing the dynamics of soil organic carbon in grasslands on the Qinghai-Tibetan Plateau. Sci. China Ser. D 50, 113–120.
Zhang, Y., Wang, G., Wang, Y., 2010. Response of biomass spatial pattern of alpine vegetation to climate change in permafrost region of the Qinghai-Tibet Plateau. China. J. Mt. Sci. 7, 301–314.
Zhang, D., Xu, W., Li, J., Cai, Z., An, D., 2014. Frost-free season lengthening and its potential cause in the Tibetan Plateau from 1960 to 2010. Theor. Appl. Climatol. 115, 441–450.
Zheng, D., 1996. The system of physico-geographical regions of the Qinghai-Xizang (Tibet) Plateau. Sci. China Ser. D 39, 410–417.
Zhong, L., Ma, Y., Salama, M.S., Su, Z., 2010. Assessment of vegetation dynamics and their response to variations in precipitation and temperature in the Tibetan Plateau. Clim. Chang. 103, 519–535.
Zhuang, Q., He, J., Lu, Y., Ji, L., Xiao, J., Luo, T., 2010. Carbon dynamics of terrestrial ecosystems on the Tibetan Plateau during the 20th century: an analysis with a process-based biogeochemical model. Glob. Ecol. Biogeogr. 19, 649–662.
Zimov, S.A., Davydov, S.P., Zimova, G.M., Davydova, A.I., Schuur, E.A.G., Dutta, K., Chapin III, F.S., 2006. Permafrost carbon: stock and decomposability of a globally significant carbon pool. Geophys. Res. Lett. 33, L20502.